ELSEVIER

Journal of Organometallic Chemistry 627 (2001) 153–158

Journal of Organometallic Chemistry

www.elsevier.nl/locate/jorganchem

Cyanide bridged oligonuclear complexes containing CuCl and $CuCl_2$

Virginie Comte, Heinrich Vahrenkamp *

Institut für Anorganische und Analytische Chemie der Universität Freiburg, Albertstr. 21, D-79104 Freiburg, Germany

Received 4 December 2000; received in revised form 17 January 2001

Dedicated to Professor Rudolf Aumann on the occasion of his 60th birthday

Abstract

The reaction between $Cp(PPh_3)_2Ru{-}CN$ and $CuCl_2$ results in $Cp(PPh_3)_2Ru{-}CN{-}CuCl$ (**1**) as the main product and $Cl(CH_3CN)(PPh_3)Ru\{CN{-}CuCl\}\{NC{-}Ru(PPh_3)_2Cp\}_2$ (**2**) as the side product. *cis*-$(bpy)_2Fe(CN)_2$ reacts with both $CuCl_2$ and CuCl to form $[(bpy)_2Fe(CN)(CN{-}CuCl_2)]_x$ (**3**) and $[(bpy)_2Fe(CN)(CN{-}CuCl)]_x$ (**4**). Upon attempts at recrystallization the former partly decomposes with formation of $(bpy)_2Fe\{CN{-}CuCl_2(bpy)\}_2$ (**5**). Electrochemical data of the complexes are reported. Complexes **1**, **2**, and **5** were identified by structure determinations. © 2001 Elsevier Science B.V. All rights reserved.

Keywords: Dinuclear, trinuclear and tetranuclear complexes; Cyanide bridging; Electrochemistry; Structures

1. Introduction

As we have outlined in the preceding publications of this series [1–8] we are trying to establish a series of oligonuclear complexes with chain-like arrangements of cyanide-bridged metal centers. The aim of this work is to find out the rules by which long range metal-metal interactions along the $(M{-}CN)_x$ chains take place. In order to do so we have varied the ligation patterns of the metallic building blocks ML_n, the geometry at the interconnected metal units (*cis*/*trans*, octahedral, tetrahedral, square-planar), and the orientation of the bridging ligand (cyanide versus isocyanide). Another important variation is the position of the metals M in the periodic table, as investigated by horizontal or vertical comparisons of similarly ligated ML_n units. In terms of these chemical variations we are mainly competing with the group of Connelly [9–12].

In this context one group of ML_n units offers itself for extensive variations, namely that of the simple metal halides $MHal_2$. Connelly has shown that quite a series of metal dihalides can be used as Lewis acids for the attachment of two metallocyanides with formation of the trinuclear complexes $Hal_2M(NC{-}M'L_n)_2$ which show a quite variable degree of metal–metal interactions between the external metal centers M′ [10–12]. We have contributed similar systems based on $NiCl_2$, $CuCl_2$, and $ZnCl_2$ [4]. During these studies we observed that $CuCl_2$ gets engaged in a redox chemistry, resulting, inter alia, in cyanide bridged complexes with terminal CuCl units. This prompted us to search for more complexes of this type, specifically trinuclear systems with a $L_mM(CN{-}CuCl_n)_2$ backbone in which metal–metal interactions between the external copper atoms might be probed by copper-centered one-electron redox interconversions.

This paper describes our first attempts in this direction. It was planned to attach both CuCl and $CuCl_2$ to metallocyanides of the type $L_nM{-}CN$ and $L_nM(CN)_2$. The latter were chosen to be $Cp(PPh_3)_2Ru{-}CN$ and *cis*-$(bpy)_2Fe(CN)_2$ of which we had experienced that they form stable and inert di- and trinuclear complexes [1,3,5,7,13]. At the same time it could be expected that the lability and redox sensitivity of the copper halides might cause redistributions and disproportionations. It turned out that both the hopes and the fears of this project were fulfilled and that $CuCl_2$ indeed promotes redox chemistry.

---

* Corresponding author. Tel.: +49-761-2036120; fax: +49-761-2036001.

E-mail address: vahrenka@uni-freiburg.de (H. Vahrenkamp).

PII: S0022-328X(01)00739-2

2. Results and discussion

2.1. Preparations

When $CuCl_2$ was treated with two equivalents of $Cp(PPh_3)_2Cu–CN$, the expected trinuclear complex was not formed. Instead, the main product was the dinuclear complex **1** in 55% yield. In addition, the workup procedure yielded a small amount (15%) of the tetranuclear complex **2**. In both products copper has been reduced to Cu(I), and **2** is the result of extensive ligand redistributions.

$Cp(PPh_3)_2Ru-CN-CuCl$
1

$Cl(CH_3CN)(PPh_3)Ru\{CN-CuCl\}\{NC-Ru(PPh_3)_2Cp\}_2$
2

Attempts to convert *cis*-$(bpy)_2Fe(CN)_2$ into a trinuclear complex by treatment with $CuCl_2$ or CuCl, as previously achieved with Cp(dppe)Fe units [13], were also only partially successful. The immediate products of these reactions, **3** and **4**, represent 1:1 combinations of Fe and Cu, as observed above for **1**. Accordingly, they were obtained in better yields (40-50%) by employing a 1:1 stoichiometry for their preparations.

$[(bpy)_2Fe(CN)(CN-CuCl_2)]_x$
3

$[(bpy)_2Fe(CN)(CN-CuCl)]_x$
4

Finally, a trinuclear $FeCu_2$ complex was obtained unexpectedly. Many attempts to obtain crystals of **3** or **4** for the elucidation of their structures were met with failure, producing **3** and **4** only as powders contaminated with decomposition products. Yet in case of **3** the decomposition product was reproducibly crystalline and could be manually separated from the powder of **3**. Its structure determination (see below) identified it as the trinuclear **5**. In **5** the terminal $CuCl_2$ units are stabilized by attachment of bpy ligands resulting from the decomposition process.

$(bpy)_2Fe\{CN-CuCl_2(bpy)\}_2$
5

2.2. Properties

The ν(CN) IR data and the redox potentials as the indicators of the electronic nature of the cyanide bridged complexes are listed in Table 1. When referenced against the data of the basic building blocks $Cp(PPh_3)_2Ru–CN$ and $(bpy)_2Fe(CN)_2$, the ν(CN) bands in all their derivatives occur at higher wavenumbers, as is to be expected due to the kinematic effect and the electron withdrawing properties of the metallic units attached at the CN's N terminus. The occurrence of two different CN units in **2**, **3** and **4** and the *cis* geometry in **5** are in accord with the occurrence of two ν(CN) bands (the single band in **4** which is just halfway between the two bands in **5** may be degenerate). Complexes **1**–**5** are too different to allow comparisons between them.

The redox potentials obtained from cyclic voltammetry are in accord with the structural assignments (see below). The Ru-centered oxidation in **1** at 1.09 V may be compared with the corresponding one in $Cp(PPh_3)_2Ru–CN–Ag–CN$ [5]. The oxidation of the CuCl unit in **1** at 1.30 V is as irreversible as that in Cp(dppe)FeCN–CuCl [4]. Both oxidations of **2** are reversible. The 2e step at 1.06 V can be assigned to the two terminal $Cp(PPh_3)_2Ru$ units while the 1e step belongs to the central ruthenium ion. Complexes **3** and **4** were not amenable to cyclic voltammetry, as was complex **5** in the reductive range. In the oxidative range, **5** shows a reversible one-electron oxidation which can be assigned to the $(bpy)_2Fe$ center.

The question of long-range electronic interactions between the external metal units in complexes **2** and **5** containing M′–CN–M–CN–M′ chains must be answerd in the negative. In **2** there is no splitting of the 2e redox wave assigned to the external $Cp(PPh_3)_2Ru$ units. In **5** reversible redox steps assignable to the external $Cu(bpy)Cl_2$ units could not be observed.

2.3. Structural assignments

For the two diamagnetic complexes **1** and **2** the NMR spectra (see Section 4) are in agreement with, yet could not be used to derive, their structures. Therefore both **1** and **2** were subjected to crystal structure determinations. The main result of the structure determination of **1** (Fig. 1) is the proof of its unexpected dinuclear nature and the presence of Cu(I). The molecular details of the $Cp(PPh_3)_2Ru–CN$ unit are well established [1–3], and there is structural precedence for **1** in both Cp(dppe)Fe–CN–CuCl [4] and Cp(dppe)Fe–CN–AgCN [5]. The simplest proof for the Ru–CN–Cu arrangement in **1** (as opposed to a Ru–NC–Cu ar-

Table 1
IR and CV data

Complex	ν(CN) [a]	$E_{1/2}$ [b]
$Cp(PPh_3)_2Ru$-CN	2072	0.79(1e)
cis-$(bpy)_2Fe(CN)_2$	2079s, 2069s	0.46(1e)
1	2089s	1.09(1e) 1.30(irrev)
2	2095s, 2080m	0.72(1e), 1.06(2e)
3	2103m, 2090s	–
4	2095s	–
5	2113s, 2096s	0.56(1e)

[a] In KBr (cm^{-1}).

[b] In CH_2Cl_2, V versus Ag/AgCl, scan rate 100 mV s^{-1}.

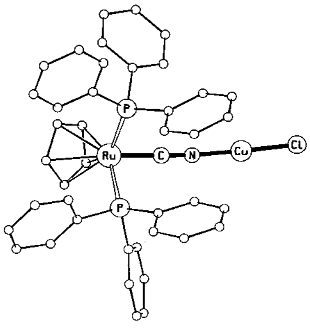

Fig. 1. Molecular structure of complex **1**. Important bond lengths (Å) and angles (°): Ru–C 1.961(5), C–N 1.168(6), N–Cu 1.810(4), Cu–Cl 2.076(2); Ru–C–N 176.9(4), C–N–Cu 171.9(4), N–Cu–Cl 178.7(1).

rangement) is the bending of the C–N–Cu angle which, as discussed in ref. [4], is a common feature distinguishing the carbon- and nitrogen-bound metal units in cyanide bridged complexes. On the other hand the ligation of copper in **1**, as that in Cp(dppe)Fe–CN–CuCl, is close to ideally linear.

The surprising molecular shape of **2** (Fig. 2) could only be obtained through the crystal structure analysis. We have previously prepared T-shaped tetrametallic complexes with M(μ-CN–M′)$_3$ arrangements [14], and facial octahedral Ru(μ-CN–M′)$_3$ complexes are known [15], but this is the first structure determination of such a species. The geometrical details of each metal unit in **2** are normal. The central Ru2 ion is almost iedeally octahedral, the copper ion is almost ideally linearly coordinated. The M–C and M–N distances are in the normal ranges and compare well with those in **1**. Typically for the central Ru2, the Ru–N distances (less backbonding) are longer than the Ru–C distance to the cyanide ligands. Except for Ru2–C3–N3 all M–C–N and M–N–C arrays are noticeably non-linear (166–172°). But again for a given M–C–N–M′ array the C–N–M′ angles are smaller than the M–C–N angles. The distance between the external ruthenium atoms is 10.4 Å, and the Ru2–Cl1 distance of 2.51 Å is unusually long. Altogether the Ru-CN–Ru–NC–Ru array compares well in terms of linearity and bond lengths with similar trimetallic arrays that we [2,3,6,7] and others [16] have described.

The structures of **3** and **4** which could not be obtained as single crystals are proposed to be as shown in Fig. 3. The proposals are based on the assumption that the cyanide attachment and the *cis* geometry of (bpy)$_2$Fe(CN)$_2$ remain unchanged. A somparison of the ν(CN) IR data can be made with similar Fe–CN–Cu species recently reported by D. Darensbourg [17]. He showed that molecular [Fe–CN–Cu–NC]$_2$ squares show two CN bands for tetrahedral copper and one CN band for trigonal copper. This agrees with the observations for **3** and **4**, and thus both can be assigned as squares as shown for **3** in Fig. 3. The distinctive difference of their solubilities causes us to propose different degrees of oligomerization for **3** and **4**, however. We assume the soluble compound **3** to be dimeric and the insoluble compound **4** to be polymeric.

The structure of complex **5** (Fig. 4) clearly shows that **5** can be derived from **3** by breaking it up by removal of one (bpy)$_2$Fe(CN)$_2$ unit and stabilizing the terminal CuCl$_2$ units by attachment of one bpy ligand each. We have described complexes of the type *cis*-(bpy)$_2$Fe(CN–ML$_n$)$_2$ before [13], but this is the first structure determination of such a complex. The iron center in **5** is octahedral to a good approximation, and its *cis*-Fe(CN)$_2$ arrangement is maintained. Proof for the Fe–C–N–Cu array lies in the bending of the Cu–N–C units again which is unusually pronounced for Cu1–N1–C1 (151°). The geometry at the copper atoms is

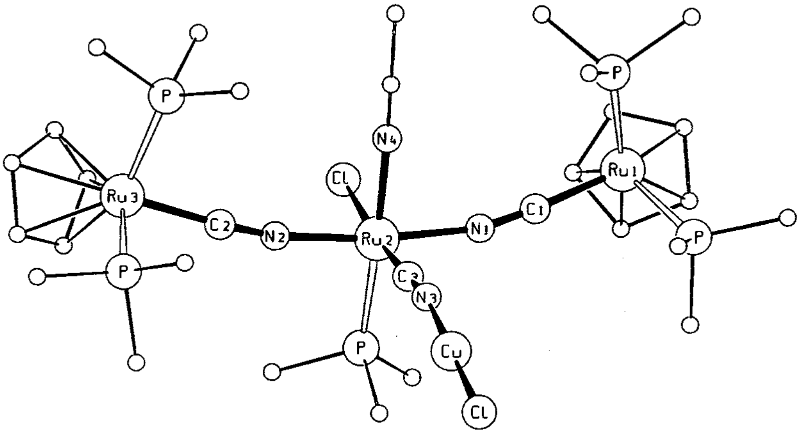

Fig. 2. Molecular structure of complex **2** (phenyl groups of the PPh$_3$ ligands omitted for clarity). Important bond lengths (Å) and angles (°): Ru1–C1 1.994(6), Ru3–C2 2.004(6), C1–N1 1.16(1), C2–N2 1.15(1), N1–Ru2 2.044(5), N2–Ru2 2.041(5), Ru2–C3 1.950(6), C3–N3 1.15(1), N3–Cu 1.833(5), Ru2–Cl1 2.506(2), Ru2–N4 2.097(5), Cu–Cl2 2.105(2); Cl1–Ru2–C3 174.3(2), N1–Ru2–N2 172.6(2), N4–Ru2–P 177.7(2), Ru1–C1–N1 171.9(5), Ru3–C2–N2 171.4(5), Ru2–N1–C1 166.9 (5), Ru2–N2–C2 169.7(5), Ru2–C3–N3 178.7(6), Cu–N3–C3 165.6(5), N3–Cu–Cl2 179.1(2).

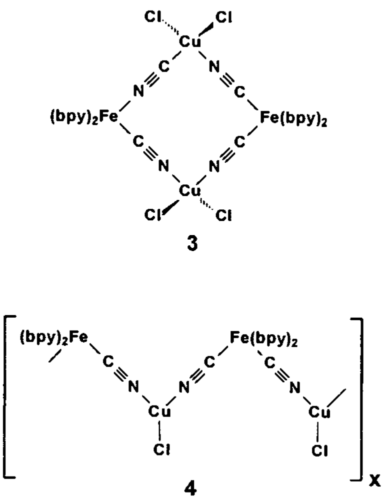

3

4

Fig. 3. Proposed structures for complexes **3** and **4**.

square-pyramidal: Cl2 at Cu1 and Cl4 at Cu2 occupy the apical positions with rather long Cu–Cl distances (2.48 Å). This is common for copper complexes with a $CuCl_2N_3$ donor set.[1] Thus, while there are no unusual features for the individual ML_n units in **5**, one aspect of its overall structure is uncommon: while other trinuclear complexes with a *cis*-M(μ-CN–M′)$_2$ arrangement take advantage of the bending at the cyanides′ C and N atoms to release steric strain between the M′ units by maximizing their distance, this is not the case here. The bending at both bridging cyanide ligands is such that the copper atoms approach one another. Their distance is 5.47 Å, markedly shorter than the value of 7.5–8 Å observed for other such complexes [3,6]. We assume that the two Cl and one bpy ligands per copper atom make the CuL_n units in **5** small enough to allow packing forces to move them toward one another.

3. Conclusions

The aim of this work was the investigation of copper containing chain-like trinuclear complexes of the types L_nM–CN–$CuCl_n$–NC–ML_n and Cl_nCu–NC–ML_n–CN–$CuCl_n$. The lability of CuCl and $CuCl_2$ both toward redox interconversions and toward ligand replacements did interfere, however, with the simple strategies of preparing such complexes from the copper chlorides and L_nM–CN or $L_nM(CN)_2$. As a result the isolated di-, tri- and tetranuclear complexes did not have the above-named simple compositions.

Dinuclear **1** has resulted from reduction of $CuCl_2$ to CuCl, which can attach only one metallocyanide ligand in a linear L_nM–CN–Cu–Cl array. The same array is present in tetranuclear **2**, but in addition during the formation of **2** one of the $Cp(PPh_3)_2Ru$–CN building blocks has undergone extensive ligand substitutions to become the central $Ru(NC)_2CN$ unit with three different additional ligands. During the formation of **3** and **4** only one $CuCl_n$ unit has been attached to the bifunctional $(bpy)_2Fe(CN)_2$ building block, but obviously it is bound to two nitrogen termini of bridging cyanide ligands, thereby making the products oligomeric. Complex **5** finally has the intended Cu–NC–Fe–CN–Cu constitution, but in order to make this array stable the copper ions are coordinated by additional bpy ligands resulting from partial decomposition of complex **3**.

The rich structural chemistry of the new complexes is a compensation for their erratic syntheses. Only binuclear **2** has simple precedence, and there are a few

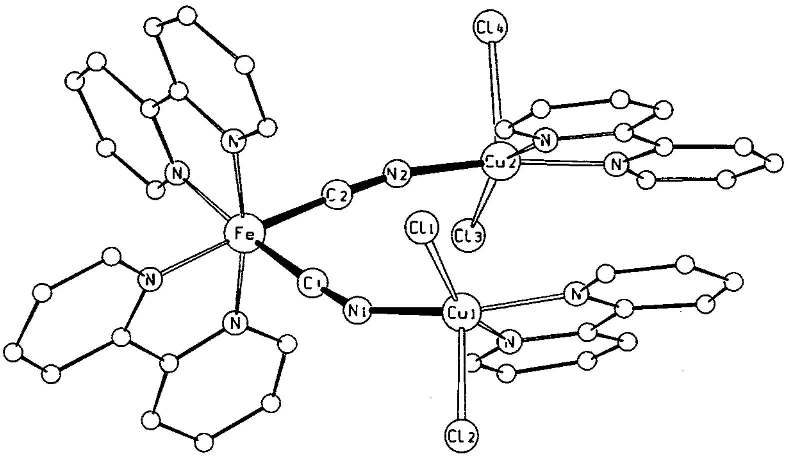

Fig. 4. Molecular structure of complex **5**. Important bond lengths (Å) and angles (°): Fe1–C1 1.91(1), Fe1–C2 1.88(1), C1–N1 1.13(1), C2–N2 1.17(1), N1–Cu1 1.98(1), N2–Cu2 1.95(1), Cu1–Cl1 2.272(3), Cu1–Cl2 2.479(3), Cu2–Cl3 2.294(3), Cu2–Cl4 2.484(3); Fe1–C1–N1 175.0(9), Fe1–C2–N2 175.5(9), C1–N1–Cu1 150.7(8), C2–N2–Cu2 168.3(9), N1–Cu1–N7 162.9(4), Cl1–Cu1–N8 153.6(3), N2–Cu2–N10 166.7(4), Cl3–Cu2–N9 155.2(3).

---

[1] The Cambridge Crystallographic Data File lists ca. 80 structures of copper complexes with a $CuCl_2N_3$ ligand set, of which a high number approximate the square-pyramidal geometry.

molecular squares like **3** and **4** in the literature [17,18]. Both the structural types of **2** and **5** are unprecedented. T-shaped complexes like **2** will be valuable for the internal comparison of 'straight-on' and 'around-the-corner' electronic interactions between the external metals in M(μ-CN)M′(μ-CN)M″ arrays [14]. And the stabilization of $CuCl_n$ units by additional ligands like in **5** shows how these units can be made amenable to a manageable redox chemistry which was the essential purpose of this study.

4. Experimental

The general experimental and measuring techniques are given in Ref. [3]. The starting materials $Cp(PPh_3)_2Ru–CN$ [19] and *cis*-$(bpy)_2Fe(CN)_2$ [20] were prepared as described.

4.1. Complex *1*

$Cp(PPh_3)_2Ru–CN$ (100 mg, 0.14 mmol) and $CuCl_2·2H_2O$ (13 mg, 0.07 mmol) in 20 ml of CH_2Cl_2 were stirred for 2 h. The solvent was removed in vacuo and 10 ml of methanol–acetonitrile (1:1) were added. The mixture was filtered and the filtrate worked up for **2** as described below. The remaining powder was washed with methanol (3 × 5 ml), dissolved in 5 ml of CH_2Cl_2 and layered with hexane. After a few days 60 mg (55%) of **1** had separated as green crystals, m.p. 240°C (dec.). ^1H-NMR (acetone-d_6): 7.3–7.1 (m, 30H, Ph), 4.47 (s, 5H, Cp). ^{31}P-NMR (acetone-d_6): 47.7 (PPh_3). Anal. Found: C, 61.31; H, 4.34; N, 1.75. Calc. for $C_{42}H_{35}ClCuNP_2Ru$ (815.76): C, 61.84; H, 4.32; N, 1.72%.

4.2. Complex *2*

The methanol–acetonitrile solution obtained during the workup for complex **1** (see above) was layered with hexane–ether (1:1). Complex **2** separated as dark green crystals (18 mg, 15%), m.p. 206°C (dec.). ^1H-NMR (acetone-d_6): 7.3–7.0 (m, 75H, Ph), 4.34 (s, 10H, Cp), 2.13 (s, 3H, CH_3CN). ^{31}P-NMR (acetone-d_6): 48.2 (s, 4P), 42.9 (s, 1P). Anal. Found: C, 64.03; H, 4.72; N, 2.65. Calc. for $C_{105}H_{88}Cl_2CuN_4P_5Ru_3$ (1998.41): C, 63.11; H, 4.44; N, 2.80%.

4.3. Complex *3*

cis-$(bpy)_2Fe(CN)_2·3H_2O$ (67 mg, 0.14 mmol) and $CuCl_2·2H_2O$ (25 mg, 0.14 mmol) in 30 ml of methanol were stirred for 4 h. The volume of the solution was reduced to 15 ml in vacuo. Upon addition of diethyl ether 80 mg (50%) of **3** were precipitated as a purple powder, m.p. 192°C. Anal. Found: C, 47.59; H, 3.06; N, 14.13. Calc. for $C_{44}H_{32}Cl_4Cu_2Fe_2N_{12}·CH_3OH$ (1109.42 + 32.04): C, 47.08; H, 3.44; N, 14.32%.

4.4. Complex *4*

cis-$(bpy)_2Fe(CN)_2$(134 mg, 0.28 mmol) and CuCl (28 mg, 0.28 mmol) were dissolved in 30 ml of acetonitrile. After a few minutes a mauve precipitate formed. After stirring for 1 h the precipitate was filtered off, washed with acetonitrile and ether and dried in vacuo. A total of 120 mg (40%) of **4** remained as a mauve powder, m.p. 190°C. Anal. Found: C, 48.95; H, 3.15; N, 16.18. Calc. for $C_{44}H_{32}Cl_2Cu_2Fe_2N_{12}$ (1038.51): C, 50.89; H, 3.11; N, 16.18%.

4.5. Complex *5*

A total of 40 mg (0.035 mmol) of **3** were dissolved with heating in 5 ml of methanol. After cooling to room temperature the solution was layered with hexane–ether (1:1) and left to stand for a week. The resulting precipitate consisted mainly of **3**, from which 7 mg (11%) of **5** were separated by hand as dark red needles, m.p. 168°C, which was identified by the structure determination.

4.6. Crystal structure determinations

Crystals of **1**, **2** and **5** were obtained as described above. The data sets were obtained with a Bruker Smart CCD diffractometer using Mo–K_α radiation. No absorption corrections were applied. The structures were solved with direct methods and refined anisotropically using the SHELX program suite [21]. Hydrogen atoms were included with a common isotropic temperature factor and a fixed C–H distance of 0.96 Å. The *R* values are defined as $R_1 = \Sigma|F_o - F_c|/\Sigma F_o$ and $wR_2 = [\Sigma[w(F_o^2 - F_c^2)^2/\Sigma[w(F_o^2)^2]]^{1/2}$. Drawings were produced with SCHAKAL [22]. Table 2 lists the crystallographic details.

5. Supplementary material

Crystallographic data for the structural analysis have been deposited with the Cambridge Crystallographic Data Centre, CCDC no. 153287 for complex **1**, CCDC no. 153288 for complex **2** and CCDC no. 153289 for complex **5**. Copies of this information may be obtained free of charge from the Director, CCDC, 12 Union Road, Cambridge, CB2 1EZ, UK (fax: +44-1223-336033; e-mail: deposit@ccdc.cam.ac.uk or http://www.ccdc.cam.ac.uk).

Table 2
Crystallographic details

	1	**2**	**5**
Crystal size (mm)	0.2 × 0.2 × 0.15	0.25 × 0.1 × 0.05	0.1 × 0.1 × 0.2
Space group	$P\bar{1}$	$P2_1/c$	$P2_1/n$
Unit cell dimensions			
a (Å)	10.950(2)	18.572(2)	9.718(1)
b (Å)	11.189(2)	22.262(3)	14.594(1)
c (Å)	14.894(3)	24.653(3)	31.231(3)
α (°)	89.23(3)	90	90
β (°)	84.66(3)	110.04(2)	90.125(2)
γ (°)	84.22(3)	90	90
Z	2	4	4
V (Å^3)	1807.8(6)	9575(2)	4429.7(7)
$D_{\text{calc.}}$ (g·cm^{-3})	1.50	1.46	1.59
μ (mm^{-1})	1.20	0.88	1.57
Reflections collected	11 570	86 486	39 708
Independent reflections $[I>2\sigma(I)]$	5193	22 635	10 711
Variables	433	1144	568
R_1 (independent reflections)	0.046	0.065	0.095
wR_2 (all reflections)	0.114	0.163	0.272
Residual el. densities	+0.8	+1.6	+0.9
Largest difference peak and hole (e Å^{-3})	−1.2	−0.9	−0.7

Acknowledgements

This work was supported by the Deutsche Forschungsgemeinschaft (Graduiertenkolleg 'Ungepaarte Elektronen').

References

[1] N. Zhu, H. Vahrenkamp, Chem. Ber. 130 (1997) 1241.
[2] A. Geiss, H. Vahrenkamp, Eur. J. Inorg. Chem. (1999) 1793.
[3] G.N. Richardson, U. Brand, H. Vahrenkamp, Inorg. Chem. 38 (1999) 3070.
[4] G.N. Richardson, H. Vahrenkamp, J. Organomet. Chem. 593 (2000) 44.
[5] V. Comte, Z.N. Chen, M.L. Flay, H. Vahrenkamp, J. Organomet. Chem. 614-615 (2000) 131.
[6] Z.N. Chen, R. Appelt, H. Vahrenkamp, Inorg. Chim. Acta 309 (2000) 65.
[7] A. Geiss, H. Vahrenkamp, Inorg. Chem. 39 (2000) 4029.
[8] A. Geiss, M.J. Kolm, C. Janiak, H. Vahrenkamp, Inorg. Chem. 39 (2000) 4037.
[9] N.C. Brown, G.B. Carpenter, N.G. Conelly, J.G. Crossley, A. Martin, A.G. Orpen, A.L. Rieger, P.H. Rieger, G.H. Worth, J. Chem. Soc. Dalton Trans. (1996) 3977, and references cited therein.
[10] N.G. Connelly, O.M. Hicks, G.R. Lewis, A.G. Orpen, A.J. Wood, J. Chem. Soc. Chem. Commun. (1998) 517.
[11] N.G. Connelly, G.R. Lewis, M.T. Moreno, A.G. Orpen, J. Chem. Soc. Dalton Trans. (1998) 1905.
[12] N.G. Connelly, O.M. Hicks, G.R. Lewis, A.G. Orpen, A.J. Wood, J. Chem. Soc. Dalton Trans. (2000) 1637.
[13] N. Zhu, H. Vahrenkamp, J. Organomet. Chem. 573 (1999) 67.
[14] G.N. Richardson, H. Vahrenkamp, J. Organomet. Chem. 597 (2000) 38.
[15] W.M. Laidlaw, R.G. Denning, Inorg. Chim. Acta 248 (1996) 51.
[16] B.J. Coe, T.J. Meyer, P.S. White, Inorg. Chem. 34 (1995) 3600.
[17] D.J. Darensbourg, W.Z. Lee, M.J. Adams, D.L. Larkins, J.H. Reibenspies, Inorg. Chem. 38 (1999) 1378.
[18] H. Oshio, H. Onodera, O. Tamada, H. Mizutani, T. Hikichi, T. Ito, Chem. Eur. J. 6 (2000) 2523.
[19] G.J. Baird, S.G. Davis, J. Organomet. Chem. 262 (1984) 215.
[20] A.A. Schildt, J. Am. Chem. Soc. 82 (1960) 3000.
[21] G.M. Sheldrick, SHELX Program Package Supplied with the Bruker Smart CCD Diffractometer.
[22] E. Keller, SCHAKAL for Windows, University of Freiburg, Germany, 1999.